Genetically Modified M13 Bacteriophage Nanonets for Enzyme Catalysis and Recovery

Vincent Mauricio Kadiri [1,2] , **Mariana Alarcón-Correa** [1] , **Jacqueline Ruppert** [1,2] ,
Jan-Philipp Günther [1,2] , **Joachim Bill** [3] , **Dirk Rothenstein** [3] **and Peer Fischer** [1,2,*]

[1] Max Planck Institute for Intelligent Systems, Heisenbergstrasse 3, 70569 Stuttgart, Germany
[2] Institute of Physical Chemistry, University of Stuttgart, Pfaffenwaldring 55, 70569 Stuttgart, Germany
[3] Institute for Materials Science, University of Stuttgart, Heisenbergstrasse 3, 70569 Stuttgart, Germany
[*] Correspondence: fischer@is.mpg.de; Tel.: +49-711-689-3560

Abstract: Enzyme-based biocatalysis exhibits multiple advantages over inorganic catalysts, including the biocompatibility and the unchallenged specificity of enzymes towards their substrate. The recovery and repeated use of enzymes is essential for any realistic application in biotechnology, but is not easily achieved with current strategies. For this purpose, enzymes are often immobilized on inorganic scaffolds, which could entail a reduction of the enzymes' activity. Here, we show that immobilization to a nano-scaled biological scaffold, a nanonetwork of end-to-end cross-linked M13 bacteriophages, ensures high enzymatic activity and at the same time allows for the simple recovery of the enzymes. The bacteriophages have been genetically engineered to express AviTags at their ends, which permit biotinylation and their specific end-to-end self-assembly while allowing space on the major coat protein for enzyme coupling. We demonstrate that the phages form nanonetwork structures and that these so-called nanonets remain highly active even after re-using the nanonets multiple times in a flow-through reactor.

Keywords: nanonets; biocatalysis; enzyme recovery; M13 bacteriophage; AviTag; enzyme immobilization

---

1. Introduction

An advantage of the use of enzymes in catalysis is their unchallenged specificity when compared to inorganic or other human-made catalysts. However, the use of enzymes in catalysis is often hindered by the difficulty in recovering the enzymes after the desired reaction has taken place. Separating the catalysts from the product solution after catalysis is essential in multiple-use reactors and particularly important if the catalyst in question is precious, hard to synthesize or extract, as is the case for many enzymes. For this purpose, the enzymes can be coupled to a scaffold or surface. The growing library of immobilization templates useful for the binding of enzymes includes many inorganic carriers, cross-linked enzyme aggregates and viruses, which can simplify the handling and recovery of enzymes.

Cross-linking enzymes to form aggregates is a straightforward and economical means to obtain larger structures from enzymes [1–7]. Furthermore, cross-linked enzyme aggregates (CLEAs) can include multiple enzymes or an additional functionality such as a magnetic property [1,7]. One major advantage offered by CLEAs is the ease of the crosslinking reactions, which in some cases only require the addition of one or two crosslinkers to obtain the final aggregate [4]. Often glutaraldehyde is chosen as a linker for these reactions. However, care must be taken when using this crosslinking strategy, as the use of glutaraldehyde might in some cases lead to a decrease in overall activity of some enzyme varieties as Sheldon [8] and Lozano et al. [4] have previously reported. To our knowledge,

there is therefore no singular CLEA platform that would work in a generally applicable manner with any enzyme.

Immobilization of an enzyme monolayer on a surface is another viable solution for recovery [9,10]. The carrier can be removed after catalysis, enabling simple separation of product solution and enzymes. While the immobilization of enzymes on inorganic surfaces is possible [11,12], it is well-known that this might lead to an activity decrease due to conformational changes or lower substrate availability [13]. It is therefore interesting to investigate immobilization of enzymes on proteinaceous environments, like viruses or virus-like particles (VLP), which can serve as scaffolds [14–21]. An attractive feature is that the viral coat-proteins are chemically addressable [16,17], allowing for the immobilization of enzymes on these naturally occurring protein-constructs. A randomly cross-linked virus nanonetwork (nanonet for short) has been demonstrated by Cuenca et. al. [14] as an enzyme scaffold using turnip mosaic viruses (TuMV) and *Candida antarctica* lipase B. The immobilization on this virus "nanonet" even led to an increase in specific enzyme activity when compared to the free enzyme, which the authors attributed to the proteinaceous environment of the virus. Nevertheless, this particular crosslinking mechanism is not specific and uses the same binding site for cross-linking and enzyme binding, which potentially reduces the available locations for catalysis.

Here, we show that nanonets can be formed using genetically modified M13 bacteriophages by linking the viruses end-to-end via an AviTag, a biotinylatable 15 amino acid (GLNDIFEAQKIEWHE) protein tag expressed as a fusion to the p3 and p7 coat proteins of the M13 bacteriophage. AviTag phages are first biotinylated by biotin ligase and the phages are subsequently cross-linked with streptavidin forming the end-to-end virus nanonets. Enzymes can be immobilized on the nanonets via the phage major coat protein p8. We show that the bacteriophage nanonets form a promising platform for heterogeneous enzyme biocatalysis. The nanonet-coupled enzymes exhibit high activity while allowing for enzyme recovery and reuse.

2. Results and Discussion

M13 bacteriophages, like other viruses, can be chemically [22,23] or genetically [24–27] addressed and modified. M13 phages are versatile, and are useful for applications including biotemplating, phage display [28–32], and even tissue regeneration, as bacteriophages are innocuous to mammalian cells [33]. Phages are highly stable in a wide range of pH and temperature conditions [34]. M13 phages are filamentous viruses, with a capsid approximately 900 nm long, and with a diameter of 6 nm. The capsid is made of five coat proteins. The main structure is formed by ~2700 copies of the major coat protein p8, which connect in a helical structure along the long axis of the virus. The coat proteins p3 and p6 form one "end" while the proteins p7 and p9 reside at the other end of the viral particle. The proteins are individually genetically modifiable and form favorable scaffolds for enzyme immobilization, as was demonstrated in our previous study of enzyme immobilization on genetically modified M13 filamentous bacteriophages [35]. Furthermore, an increase in enzymatic activity when coupled to a proteinaceous substrate was demonstrated in that study as well as by others [14,35,36]. Here, we show that a phage nanonetwork can be obtained using genetically modified M13 bacteriophages designed to specifically self-assemble end-to-end. We then demonstrate that the nanonet is an easily modifiable platform for enzyme immobilization and repeated enzyme recovery.

2.1. Biotinylation and Characterization of M13 Bacteriophages

The general scheme to prepare the nanonets is shown in Figure 1. The sequencing data shows that the genetic modification of M13 bacteriophages for the expression of the AviTag fusion protein was successful (Supplementary Materials). We produced viruses with the AviTag proteins fused to the p3 and p7 proteins (p3p7 AviTag phages), as well as phages modified either with AviTags only at p3 proteins (p3 AviTag phages) or only at the p7 proteins (p7 AviTag phages). The p3p7 AviTag phages were biotinylated (Figure 1a) as previously reported [14,24–27] using a modification of the method described by Litvinov et al. [26]. Briefly, p3p7 AviTag phages were incubated with biotin ligase, biotin,

ATP, bicine and magnesium acetate. After a PEG/NaCl cleanup, a sample of the now biotinylated bacteriophages (p3p7 B phages) was obtained. After biotinylation, the phage concentration in the solution was ~10^{15} pfu/mL, as determined by UV-Vis absorption spectroscopy. At this point, it is worth mentioning that the absorption of biotin at 269 nm in the UV-Vis, shown in Figure S1a, was negligible. To determine the yield and confirm the biotinylation of p3p7 B phages, a small volume fraction of the solution was diluted and incubated with an excess of streptavidin-coated magnetic colloids. Only 20% of p3p7 B phages remained in solution, suggesting that 80% of p3p7 B phages bound to the streptavidin-colloids and successfully presented biotin. For comparison, only 7% of un-biotinylated p3p7 AviTag phages and 26% of wild type phages without any AviTags were found to bind to the streptavidin beads (Figure S1b). We also quantified the biotinylation yield of p3 B phages and p7 B phages using the streptavidin-colloids. On average, phages with a modified p3 exhibited a higher binding yield (89%) than those in which the modification was on the p7 protein (63%). The remaining 11% and 37%, respectively, had therefore either not been biotinylated by the biotin ligase or the biotin was not accessible to the streptavidin-colloids. We speculate that the higher affinity of the p3 B phages to the streptavidin-colloids, when compared to the p7 B phages, might thus be due to higher accessibility of either the fused AviTag peptide during biotinylation or of the biotin in p3 position after biotinylation and is consistent with results previously seen in the literature [27].
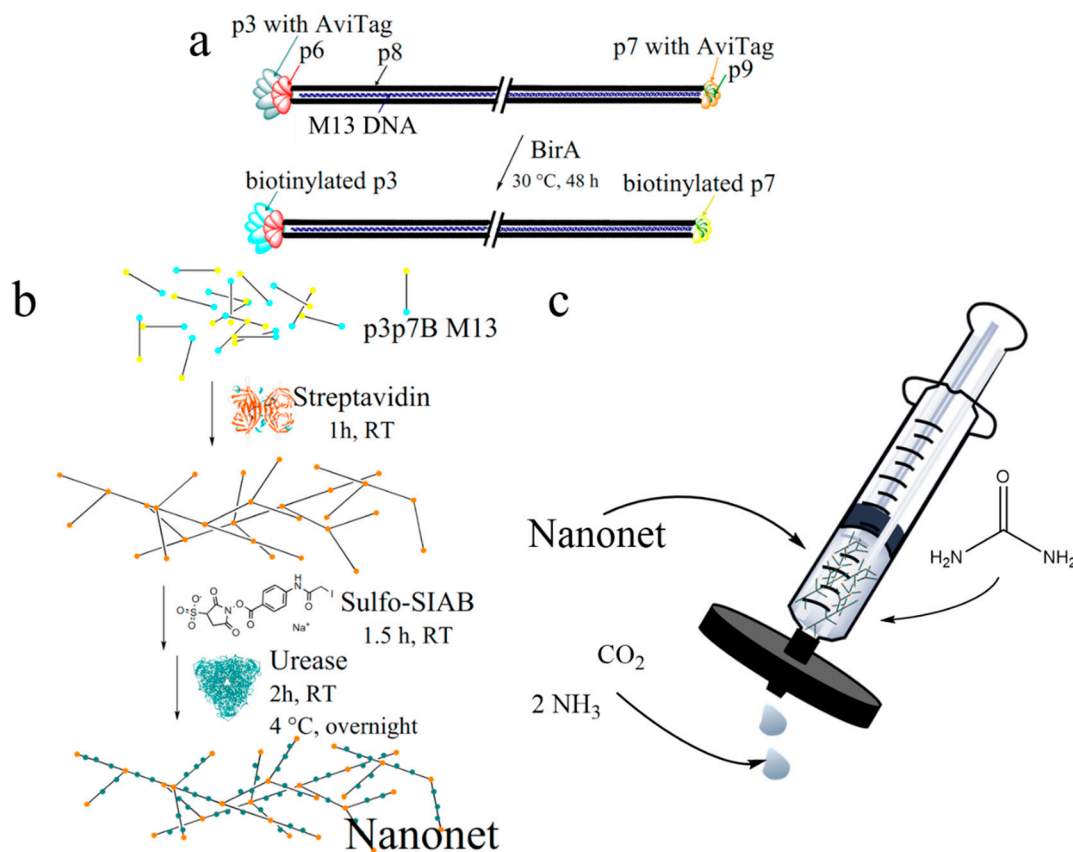
Figure 1. Illustrations of (**a**) fabrication of M13 bacteriophages biotinylated on the p3 and p7 coat proteins (p3p7 B phages) and (**b**) fabrication of urease–bacteriophage nanonet. (**c**) Illustration of the use of nanonet as a low cost, small flow-through reactor using a syringe filter.

2.2. Nanonet Synthesis and Characterization

After determining the concentration and yield of p3p7 B phages by UV-Vis, a two-fold excess of streptavidin (STV) was added to the phages and after incubation, a viscous liquid was obtained. We assume that the "mesh size" of a network of end-to-end coupled phages (nanonets) is relatively large since the solution is still fairly liquid and not gelatinous. In order to visualize the formation of

network structures, p3p7 B phages were functionalized with an ALEXA 488 NHS-ester (see Materials and Methods section) and diluted to 10^{11} pfu/mL to facilitate imaging with fluorescence microscopy (see Supporting Video 1). When these diluted ALEXA 488-labelled p3p7B M13 were incubated with a two-fold excess of streptavidin, agglomerates with a diameter of up to 25 µm were clearly visible, suggesting that phage constructs formed. When adding streptavidin to un-biotinylated p3p7 AviTag phages or wild type M13, agglomeration was not observed.

The nanonets were then functionalized with urease, an enzyme whose activity and stability is readily tracked by a colorimetric activity assay. After coupling urease to the cross-linked phages via the bifunctional linker sulfo-SIAB the stability of the urease–sulfo-SIAB nanonets, further referred to as enzyme-nanonets, increased and agglomerates with a diameter of up to 2 mm formed (Figure 2a, Supporting Video 2). The macroscopic enzyme-nanonets are mechanically stable and can be picked up with a spatula (see Supporting Video 3). Electron micrographs and analysis of the dried nanonets showed dense agglomerates made of p3p7 B phages (Figure S2).
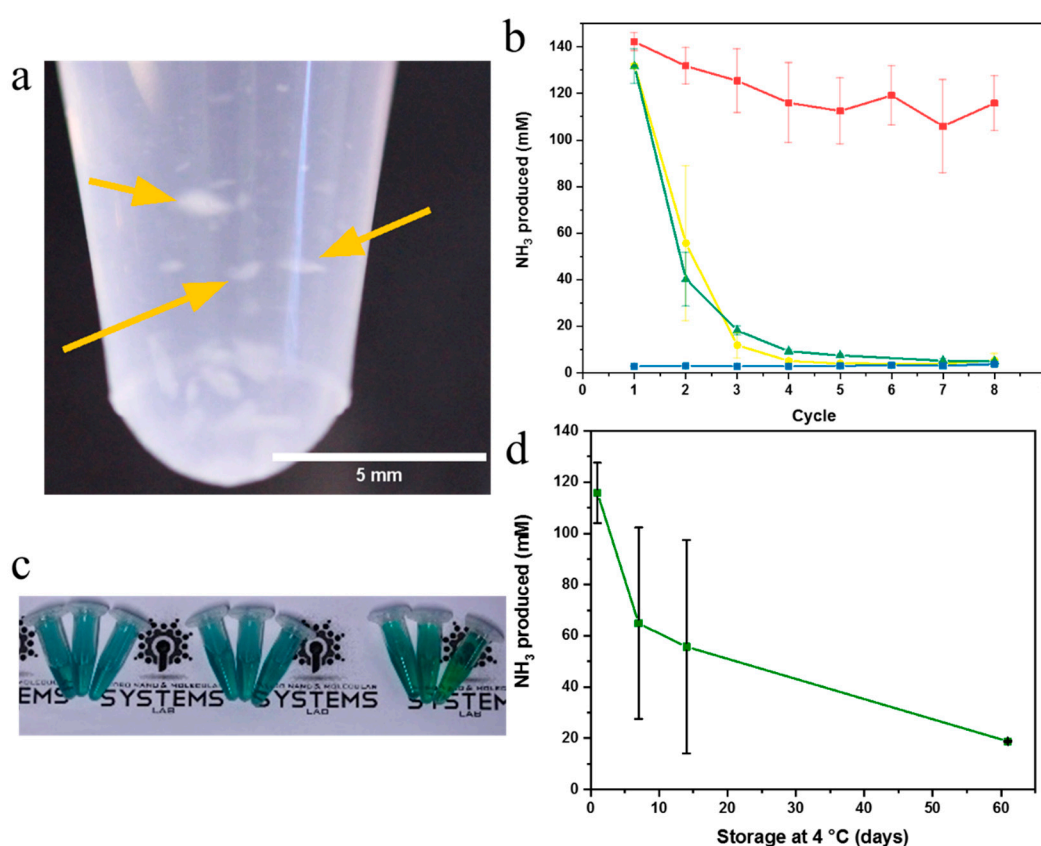
Figure 2. (**a**) Macroscopic urease-sulfo-SIAB-streptavidin-nanonet (enzyme-nanonets). (**b**) Urease activity test showing ammonia production over 5 minutes as a function of repeated recovery (via centrifugation) of free urease (yellow), enzyme-nanonets (red), as well as urease cross-linked to p3p7 AviTag phages using (i) Sulfo-SIAB (green); and (ii) glutaraldehyde (blue). (**c**,**d**) Comparison of long term stability of enzymatic activity over 2 months of storage at 4 °C for different enzyme-nanonets. Error bars for all graphs were obtained through a minimum of three repetitions.

2.3. Enzyme Activity Assays of Nanonets

To determine whether the immobilized enzymes retained their activity, a variant of the Berthelot colorimetric assay, introduced by Verdouw et al. [37], was utilized. The method permits quantification of substrate conversion by observing the amount of blue-green indophenol derivate that is produced in the reaction (Figure S3). We tracked the peak shift in the absorption spectrum to calculate activities. Our measurements showed high urease activity for the enzyme-nanonets. Figure 2b shows the urease

activity by tracking the decomposition of urea to ammonia. After the reaction, the enzyme-nanonets could easily be recovered by centrifugation for 5 min at 14,500 g and thus repeatedly used. We observed a conversion rate of 2.8 ± 0.1 µmol/min ammonia over 5 min for the enzyme-nanonets in the first reaction solution. A drop in activity after the first use was exhibited by all samples. This is most likely caused by the loss of unspecifically or weakly bound enzymes and phages. Importantly, no significant decrease in the amount of substrate turnover was measured for the enzyme-nanonets following further recovery steps resulting in a residual activity of 2.3 ± 0.2 µmol/min after eight cycles, i.e., 82% of activity being retained. In contrast, the free enzymes and the urease coupled to non-cross-linked p3p7 AviTag phages exhibited a steady decrease in activity every time the enzymes were reused (Figure 2b, Figure S4). Here, after eight cycles, the remaining activity was 0.10 ± 0.06 µmol/min, corresponding to about one-thirtieth of the initial activity for free enzymes (and 0.10 ± 0.01 µmol/min for urease coupled to non-cross-linked p3p7 AviTag phages). The colorimetric assays pictured in Figure S4 further illustrate the stability of the nanonets when compared with unbound enzymes, non-cross-linked p3p7 AviTag phages and unspecifically cross-linked nanonets using glutaraldehyde (Supporting Information 6). As observed in UV-Vis, the two former control samples show a very strong decrease in activity over the first two cycles, most likely due to loss of enzymes and or phages from one step to the next. The sample with glutaraldehyde as cross-linker exhibits a lowered activity from the start. We also studied the activity of our nanonets after long-term storage, to show that the proteinaceous environment, on which the enzymes are immobilized, is favorable for the enzymes. The nanonets retained half of their initial activity over the course of two weeks and one eighth after 2 months (Figure 2c) when stored at 4 °C.

2.4. Syringe Filter Nanonet Reactor

A key advantage of the nanonets is that they can be reused by being transferred from one reaction container to the next (without the need for centrifugation), as can be seen in Supporting Video 3, and thus reduce the amount of enzymes required for repeated catalysis. Nevertheless, the enzyme-nanonets are mechanically fragile which prevents their repeated use without loss of material. However, loss of material can easily be avoided if a 100 nm syringe filter is used as support for the enzyme-nanonets, as illustrated in Figure 1c. The filter holds the enzyme-nanonet back while allowing the substrate solution to pass through. Retention of the enzyme-nanonet is easily achieved with the use of a commercial 100 nm filter (Figure S5a). To determine the activity of the nanonets on the filter, the urea solution was passed through the filter. After regular intervals, the activity was measured by a colorimetric assay. No measurable decrease in the nanonet enzymatic activity could be observed, as reported in Figure 3a,b. Free enzyme on the other hand showed a drastic decline in the amount of ammonia produced as the fluid is flushed through the filter, which suggests that the enzymes must either become less active on the filter or pass through the filter themselves.

In fact, we determined that 40% of the free enzymes pass through the filter after filtering a solution of urease (Figure S5a). The nanonets thus perform an essential function, as the free enzyme or non-cross-linked p3p7 AviTag phages easily pass through the filter. On the other hand, for the enzyme-nanonets, the retention dramatically increases to 96%. We speculate that the remaining 4% that pass through the filter are smaller units of uncoupled phages and enzymes. Macroscopic nanonets like the ones pictured in Figure 2a were found to be retained by 100 nm syringe filters (Figure S5b,c). Even though 60% of urease should be retained by the filter, the enzymes nevertheless are seen to lose activity. This might be due to loss of conformation of the enzymes in contact with the filter material. For the urease immobilized on the nanonet, on the other hand, the enzymatic activity remains stable on the syringe filter (Figure 3a.b), which further illustrates that the nanonet and with it the enzymes can be successfully recovered without significant loss in activity due to the immobilization. The urease coupled to the enzyme-nanonet, in contrast to the free enzyme, can thus be reused when utilizing this inexpensive flow-through "nanoreactor".
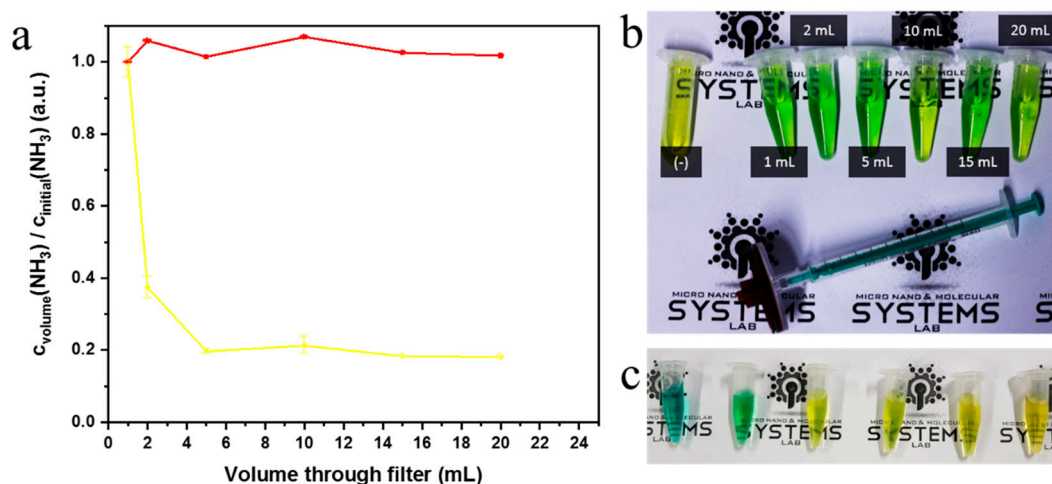
Figure 3. (**a**) Urease activities (normalized by initial activities) as a function of volume passed through nanonet filter for enzyme nanonets (red) and free enzyme (yellow). (**b**) Syringe filter setup with nanonet filter and representative samples corresponding to red line in graph (**a**) as well as a negative sample (-). (**c**) Colorimetric assay samples corresponding to yellow line in graph (**a**). Error bars for all graphs were obtained through a minimum of three repetitions.

3. Materials and Methods

3.1. Materials

The genetic modification to obtain AviTag M13 bacteriophages is described in the Supplementary Materials. Bicine buffer (1 M) was purchased from Jena Bioscience, Germany. ALEXA Fluor 488 NHS Ester, Dynabeads MyOne Streptavidin C1, Gibco PBS tablets (pH 7.4), and sulfosuccinimidyl (4-iodoacetyl) aminobenzoate (Sulfo-SIAB) were purchased from Thermo Fisher Scientific, Schwerte Germany. Sodium chloride was purchased from Carl Roth, Karlsruhe, Germany. Sodium hypochlorite solution (10%) was purchased from Fluka Analytical, Munich, Germany. Magnesium acetate tetrahydrate was purchased from Santa Cruz Biotechnology. Disodium adenosine 5'-triphosphate (ATP, 99%), biotin ligase (BirA, recombinant, ≥65%), carbamide, D-biotin (≥99% lyophilized powder), bovine serum albumin (≥96%, lyophilized powder), 25% glutaraldehyde, poly(ethylene glycol) methyl ether (PEG, 5000 Da), sodium hydroxide, sodium nitroprusside dihydrate, sodium salicylate, streptavidin (recombinant, lyophilized powder), urease (from *Canavalia ensiformis* (Jack bean) Type C-3, 120 ± 10 mg of urease per 1 g powder [35]) were purchased from Sigma-Aldrich, Munich, Germany. All chemicals were used as purchased unless otherwise specified.

3.2. M13 Bacteriophage Biotinylation

AviTag phages were stored in 1 x TBS (50 mM Tris-Cl, pH 7.6; 150 mM NaCl) buffer at 4 °C and were used at concentrations of 10^{15} pfu/mL unless stated otherwise. Four microliters of 500 mM biotin, 4 μL ATP solution (100 mM ATP, 500 mM biotin, and 100 mM magnesium acetate) and 4 μL 0.5 M bicine were mixed with 100 μL of a p3p7 AviTag phage stock solution. Then, 20 μL of 2 mg/mL biotin ligase was thoroughly mixed in and the solution was allowed to react in a shaker (600 rpm) for at least 48 h at 30 °C. To recover the phages from the reaction solution, 30.5 μL of a 2.5 M sodium chloride in 20% poly (ethylene glycol) solution were added and the solution was cooled for 20 min in an ice bath followed by centrifugation at 16,200 g for 20 min at 4 °C. The supernatant was removed and the pellet containing the phages was re-suspended in 100 μL 1x PBS, pH 7.4. This PBS buffer was used in all subsequent steps.

3.3. Characterization of Biotinylation Yield of M13 Bacteriophage

Two microliters of p3p7 biotinylated M13 bacteriophages were diluted in 278 μL PBS buffer. The concentration of the M13 phage solution was determined by using 140 μL of the stock solution to measure the UV-Vis absorption at 269 nm and at 320 nm as described by Smith [38]. The phages of the remaining solution were immobilized on magnetic streptavidin beads (Dynabeads MyOne Streptavidin C1, Invitrogen) [39]. Briefly, 100 μL of MyOne C1 Dynabeads solution was placed on a small lab magnet for 2 min to concentrate the beads at the bottom of a reaction tube. The supernatant was discarded and 300 μL PBS buffer was added. This washing step was repeated three times. The Dynabeads were then pulled to the bottom of the reaction tube once more with the magnet and, after removing the supernatant, the phage solution (140 μL) was added and incubated at room temperature for at least 1 h on a shaker at 600 rpm. After immobilization, the supernatant was removed and the UV-Vis absorbance of the supernatant was measured to calculate concentration of the unbound phages.

3.4. M13 Bacteriophage Nanonet

The equivalent of two streptavidin (STV) moieties per phage was added to 100 μL of p3p7 biotinylated M13 phages as a 1 mg/mL STV solution. The resulting viscous solution was used without further purification.

3.5. Sulfo-SIAB Cross-Linked Urease Nanonet (Enzyme-Nanonets)

Ten microliters of the M13 bacteriophage nanonet was suspended in 1 mL PBS buffer and incubated on a shaker at 600 rpm with 300 μL of a sulfo-SIAB solution (3 mg/mL in PBS) for 1.5 h at room temperature. The solution was then centrifuged in a benchtop microcentrifuge at 14,000 g for 5 min. After discarding the supernatant, 500 μL of a fresh 5 mg/mL urease solution was added to the pellet. The pellet was then carefully re-suspended and incubated at room temperature in the dark for 2 h while shaking at 600 rpm. The nanonets were stored at 4 °C overnight before use.

3.6. Glutaraldehyde Cross-Linked Urease Nanonet

The crosslinking procedure has been modified based on Cuenca et al. [14]. In particular, 500 μL of a 5 mg/mL urease solution was incubated with 1% glutaraldehyde (GA) for 1 h. The excess glutaraldehyde was cleared with the help of a centrifugal 10 kDa MWCO filter (Merck Millipore, Darmstadt, Germany). 1 mL of 10^{13} pfu/mL M13 bacteriophages solution was then added to the GA-activated urease solution and incubated overnight on a shaker at 600 rpm.

3.7. Fluorescence Imaging

For fluorescence imaging of the biotinylated bacteriophages, 10 μL of a 10^{13} pfu/mL solution was incubated with 10 μL 4 mM ALEXA 488 for 1 h at room temperature (stirring at 700 rpm). After incubation, 780 μL PBS buffer was added and the solution was dialyzed in PBS (Spectrum Labs, Float-A-Lyzer G2 300 kDa) with four buffer exchanges. Ten microliters of the dialyzed phage solution was incubated 2:1 with streptavidin. The phages were imaged in a Zeiss Axiovert inverted microscope with a 100× oil immersion objective on bovine serum albumin-coated glass cover slides.

3.8. Urease Activity Assays

The nanonets were centrifuged at 14,500 g for 5 min, the supernatant discarded, and 100 μL of a 500 mM urea solution (in PBS buffer at pH 7.4) was added. The reaction mixture was centrifuged for another 5 min. The supernatant was removed and 550 μL of a 5 mM solution of sodium nitroprusside, 60 mM sodium salicylate and 400 μL of a 400 mM sodium hydroxide, 10 mM sodium hypochlorite solution were added to it. The resultant mixture was incubated until no further color change could be observed (<30 min). For re-cycling the nanonets, the nanonets were pelleted and re-suspended as described above.

3.9. Syringe Filter Reactor

The enzyme-nanonets were synthesized as described and re-suspended in 1 mL PBS buffer. The dispersion was drawn into a 1 mL syringe (NORM-JECT Luer Lock, VWR, Darmstadt, Germany) and passed through a commercial 100 nm syringe filter (PES 0.1 μm Sartorius, Göttingen, Germany). To determine the enzymatic activity, 500 mM urea suspended in PBS buffer was run through the filter, 200 μL samples were collected after, respectively, 1, 2, 5, 10, 15, and 20 mL have passed the filter. The activity assay was then performed on these samples as described above. To determine how many phages passed through the filter, nanonets were placed on the filter surface and 20 mL PBS was flushed through the filter. Fractions of the solution after filtration were then collected after every 2 mL and the concentration of the remaining phages determined via UV-Vis as described above.

4. Conclusions

In summary, we have shown that genetically engineered M13 bacteriophages can be used to construct catalytically active enzyme–virus nanonets. The phages offer a proteinaceous template onto which enzymes can readily be coupled and on which enzymes retain their activity. The enzyme-decorated nanonets presented here not only outperformed analogous methods of creating viral nanonets in terms of activity but also allow for simple recovery of the enzymes after use. Enzyme recovery in biocatalysis is generally challenging, but we show that centrifugation for 5 minutes or the use of a syringe filter are sufficient methods to recover the enzyme-nanonets, and hence the enzymes. When compared to solutions with unbound enzymes, it becomes clear that the enzyme-nanonets can easily be used several times. We were able to show, that the enzyme-nanonets remained active for at least 2 months when stored at 4 °C. Using the enzyme-nanonets, we have successfully built a continuous flow-through "nanoreactor" for enzyme catalysis. The phages and the coupling scheme are versatile and so the method we demonstrate can also be expanded to be used with other enzymes. Even multiple enzymes can potentially be immobilized, which may be of interest in cascade reactions.

Supplementary Materials: The following are available online at http://www.mdpi.com/2073-4344/9/9/723/s1, Figure S1: UV-vis spectra and biotinylation yield, Figure S2: Macroscopic nanonet, Figure S3: Colorimetric assays and calibration curve for determination of enzyme activity, Figure S4: Urease activity assays over multiple centrifugation cycles, Figure S5: Retention of phages. Supporting Video 1.mp4, Supporting Video 2.mp4, Supporting Video 3.mp4.

Author Contributions: The manuscript was written with contributions of all authors. V.M.K. and P.F. conceptualized the study; V.M.K., J.R. and D.R. performed investigations; V.M.K. analyzed, compiled and visualized the data; V.M.K., M.A.-C. and P.F. wrote the original draft; all authors critically reviewed and edited the manuscript; J.B., D.R. and P.F. supervised the project and acquired funding. All authors have given approval to the final version of the manuscript.

Funding: This work was in part supported by the Volkswagen Stiftung under the project "Self-assembled nano-reactors via bacteriophage engineering (ROBOPHAGE)", the DFG as part of the project SPP 1726 (microswimmers, 253407113), and the Max Planck Society.

Acknowledgments: Parts of the Figures were based on molecular graphics and analyses performed with UCSF Chimera 1.13.1 [40], developed by the Resource for Biocomputing, Visualization, and Informatics at the University of California, San Francisco, United States.

Conflicts of Interest: The authors declare no conflict of interest.

References

1.　Lucena, G.N.; dos Santos, C.C.; Pinto, G.C.; da Rocha, C.O.; Brandt, J.V.; de Paula, A.V.; Jafelicci Júnior, M.; Marques, R.F.C. Magnetic cross-linked enzyme aggregates (MCLEAs) applied to biomass conversion. *J. Solid State Chem.* **2019**, *270*, 58–70. [CrossRef]

2.　Sheldon, R.A.; Schoevaart, R.; Van Langen, L.M. Cross-linked enzyme aggregates (CLEAs): A novel and versatile method for enzyme immobilization (a review). *Biocatal. Biotransform.* **2005**, *23*, 141–147. [CrossRef]

3. Touahar, I.E.; Haroune, L.; Ba, S.; Bellenger, J.-P.; Cabana, H. Characterization of combined cross-linked enzyme aggregatès from laccase, versatile peroxidase and glucose oxidase, and their utilization for the elimination of pharmaceuticals. *Sci. Total Environ.* **2014**, *481*, 90–99. [CrossRef] [PubMed]

4. Velasco-Lozano, S.; López-Gallego, F.; Mateos-Díaz Juan, C.; Favela-Torres, E. Cross-linked enzyme aggregates (CLEA) in enzyme improvement—A review. *Biocatalysis* **2016**, *1*, 166–177. [CrossRef]

5. Xu, M.-Q.; Wang, S.-S.; Li, L.-N.; Gao, J.; Zhang, Y.-W. Combined cross-linked enzyme aggregates as biocatalysts. *Catalysts* **2018**, *8*, 460. [CrossRef]

6. Zhang, Q.; Zha, X.; Zhou, N.; Tian, Y. Preparation of crosslinked enzyme aggregates (CLEAs) of acid urease with urethanase activity and their application. *J. Basic Microbiol.* **2016**, *56*, 422–431. [CrossRef]

7. Sheldon, R.A. CLEAs, Combi-CLEAs and 'Smart'Magnetic CLEAs: Biocatalysis in a Bio-Based Economy. *Catalysts* **2019**, *9*, 261. [CrossRef]

8. Sheldon, R.A. Characteristic features and biotechnological applications of cross-linked enzyme aggregates (CLEAs). *Appl. Microbiol. Biotechnol.* **2011**, *92*, 467–477. [CrossRef]

9. Cao, L.; Langen, L.; Sheldon, R.A. Immobilised enzymes: Carrier-bound or carrier-free? *Curr. Opin. Biotechnol.* **2003**, *14*, 387–394. [CrossRef]

10. Sheldon, R.A. Enzyme Immobilization: The Quest for Optimum Performance. *Adv. Synth. Catal.* **2007**, *349*, 1289–1307. [CrossRef]

11. Magne, V.; Amounas, M.; Innocent, C.; Dejean, E.; Seta, P. Enzyme textile for removal of urea with coupling process: Enzymatic reaction and electrodialysis. *Desalination* **2002**, *144*, 163–166. [CrossRef]

12. Mohamad, N.R.; Marzuki, N.H.C.; Buang, N.A.; Huyop, F.; Wahab, R.A. An overview of technologies for immobilization of enzymes and surface analysis techniques for immobilized enzymes. *Biotechnol. Biotechnol. Equip.* **2015**, *29*, 205–220. [CrossRef] [PubMed]

13. Garcia-Galan, C.; Berenguer-Murcia, Á.; Fernandez-Lafuente, R.; Rodrigues, R.C. Potential of Different Enzyme Immobilization Strategies to Improve Enzyme Performance. *Adv. Synth. Catal.* **2011**, *353*, 2885–2904. [CrossRef]

14. Cuenca, S.; Mansilla, C.; Aguado, M.; Yuste-Calvo, C.; Sánchez, F.; Sánchez-Montero, J.M.; Ponz, F. Nanonets Derived from Turnip Mosaic Virus as Scaffolds for Increased Enzymatic Activity of Immobilized Candida antarctica Lipase B. *Front. Plant Sci.* **2016**, 7. [CrossRef] [PubMed]

15. Cardinale, D.; Carette, N.; Michon, T. Virus scaffolds as enzyme nano-carriers. *Trends Biotechnol.* **2012**, *30*, 369–376. [CrossRef] [PubMed]

16. Hooker, J.M.; Kovacs, E.W.; Francis, M.B. Interior Surface Modification of Bacteriophage MS2. *J. Am. Chem. Soc.* **2004**, *126*, 3718–3719. [CrossRef] [PubMed]

17. Arora, P.S.; Kirshenbaum, K. Nano-Tailoring: Stitching Alterations on Viral Coats. *Chem. Biol.* **2004**, *11*, 418–420. [CrossRef] [PubMed]

18. Comellas-Aragonès, M.; Engelkamp, H.; Claessen, V.I.; Sommerdijk, N.A.J.M.; Rowan, A.E.; Christianen, P.C.M.; Maan, J.C.; Verduin, B.J.M.; Cornelissen, J.J.L.M.; Nolte, R.J.M. A virus-based single-enzyme nanoreactor. *Nat. Nanotechnol.* **2007**, *2*, 635. [CrossRef] [PubMed]

19. Röder, J.; Fischer, R.; Commandeur, U. Engineering Potato Virus X Particles for a Covalent Protein Based Attachment of Enzymes. *Small* **2017**, *13*, 1702151. [CrossRef]

20. Eiben, S.; Koch, C.; Altintoprak, K.; Southan, A.; Tovar, G.; Laschat, S.; Weiss, I.M.; Wege, C. Plant virus-based materials for biomedical applications: Trends and prospects. *Adv. Drug Deliv. Rev.* **2018**. [CrossRef]

21. Carette, N.; Engelkamp, H.; Akpa, E.; Pierre, S.J.; Cameron, N.R.; Christianen, P.C.M.; Maan, J.C.; Thies, J.C.; Weberskirch, R.; Rowan, A.E.; et al. A virus-based biocatalyst. *Nat. Nanotechnol.* **2007**, *2*, 226. [CrossRef] [PubMed]

22. Li, K.; Chen, Y.; Li, S.; Nguyen, H.G.; Niu, Z.; You, S.; Mello, C.M.; Lu, X.; Wang, Q. Chemical modification of M13 bacteriophage and its application in cancer cell imaging. *Bioconjug. Chem.* **2010**, *21*, 1369–1377. [CrossRef] [PubMed]

23. Mohan, K.; Weiss, G.A. Chemically Modifying Viruses for Diverse Applications. *ACS Chem. Biol.* **2016**, *11*, 1167–1179. [CrossRef] [PubMed]

24. Adhikari, M.; Strych, U.; Kim, J.; Goux, H.; Dhamane, S.; Poongavanam, M.-V.; Hagström, A.E.V.; Kourentzi, K.; Conrad, J.C.; Willson, R.C. Aptamer-Phage Reporters for Ultrasensitive Lateral Flow Assays. *Anal. Chem.* **2015**, *87*, 11660–11665. [CrossRef] [PubMed]

25. Adhikari, M.; Dhamane, S.; Hagstrom, A.E.V.; Garvey, G.; Chen, W.-H.; Kourentzi, K.; Strych, U.; Willson, R.C. Functionalized viral nanoparticles as ultrasensitive reporters in lateral-flow assays. *Analyst* **2013**, *138*, 5584–5587. [CrossRef]

26. Litvinov, J.; Hagström, A.E.V.; Lopez, Y.; Adhikari, M.; Kourentzi, K.; Strych, U.; Monzon, F.A.; Foster, W.; Cagle, P.T.; Willson, R.C. Ultrasensitive immuno-detection using viral nanoparticles with modular assembly using genetically-directed biotinylation. *Biotechnol. Lett.* **2014**, *36*, 1863–1868. [CrossRef]

27. Smelyanski, L.; Gershoni, J.M. Site directed biotinylation of filamentous phage structural proteins. *Virol. J.* **2011**, *8*, 495. [CrossRef]

28. Rothenstein, D.; Claasen, B.; Omiecienski, B.; Lammel, P.; Bill, J. Isolation of ZnO-Binding 12-mer Peptides and Determination of Their Binding Epitopes by NMR Spectroscopy. *J. Am. Chem. Soc.* **2012**, *134*, 12547–12556. [CrossRef]

29. Rothenstein, D.; Shopova-Gospodinova, D.; Bakradze, G.; Jeurgens, L.P.H.; Bill, J. Generation of luminescence in biomineralized zirconia by zirconia-binding peptides. *CrystEngComm* **2015**, *17*, 1783–1790. [CrossRef]

30. Kilper, S.; Facey, S.J.; Burghard, Z.; Hauer, B.; Rothenstein, D.; Bill, J. Macroscopic Properties of Biomimetic Ceramics Are Governed by the Molecular Recognition at the Bioorganic–Inorganic Interface. *Adv. Funct. Mater.* **2018**, *28*, 1705842. [CrossRef]

31. Kilper, S.; Jahnke, T.; Aulich, M.; Burghard, Z.; Rothenstein, D.; Bill, J. Genetically Induced In Situ-Poling for Piezo-Active Biohybrid Nanowires. *Adv. Mater.* **2019**, *31*, 1805597. [CrossRef] [PubMed]

32. Bruin, R.d.; Spelt, K.; Mol, J.; Koes, R.; Quattrocchio, F. Selection of high-affinity phage antibodies from phage display libraries. *Nat. Biotechnol.* **1999**, *17*, 397–399. [CrossRef] [PubMed]

33. Merzlyak, A.; Indrakanti, S.; Lee, S.-W. Genetically Engineered Nanofiber-Like Viruses For Tissue Regenerating Materials. *Nano Lett.* **2009**, *9*, 846–852. [CrossRef] [PubMed]

34. Branston, S.D.; Stanley, E.C.; Ward, J.M.; Keshavarz-Moore, E. Determination of the survival of bacteriophage M13 from chemical and physical challenges to assist in its sustainable bioprocessing. *Biotechnol. Bioprocess Eng.* **2013**, *18*, 560–566. [CrossRef]

35. Alarcón-Correa, M.; Günther, J.-P.; Troll, J.; Kadiri, V.M.; Bill, J.; Fischer, P.; Rothenstein, D. Self-Assembled Phage-Based Colloids for High Localized Enzymatic Activity. *ACS Nano* **2019**, *13*, 5810–5815. [CrossRef] [PubMed]

36. Koch, C.; Wabbel, K.; Eber, F.J.; Krolla-Sidenstein, P.; Azucena, C.; Gliemann, H.; Eiben, S.; Geiger, F.; Wege, C. Modified TMV Particles as Beneficial Scaffolds to Present Sensor Enzymes. *Front. Plant Sci.* **2015**, *6*, 1137. [CrossRef] [PubMed]

37. Verdouw, H.; Van Echteld, C.J.A.; Dekkers, E.M.J. Ammonia determination based on indophenol formation with sodium salicylate. *Water Res.* **1978**, *12*, 399–402. [CrossRef]

38. Smith, G.P. Absorption Spectrum and Quantitation of Filamentous Phage. Available online: http://www.biosci. missouri.edu/smithgp/PhageDisplayWebsite/PhageDisplayWebsiteindex.html (accessed on 26 August 2019).

39. Scholle, M.D.; Kriplani, U.; Pabon, A.; Sishtla, K.; Glucksman, M.J.; Kay, B.K. Mapping Protease Substrates by Using a Biotinylated Phage Substrate Library. *ChemBioChem* **2006**, *7*, 834–838. [CrossRef] [PubMed]

40. Pettersen, E.F.; Goddard, T.D.; Huang, C.C.; Couch, G.S.; Greenblatt, D.M.; Meng, E.C.; Ferrin, T.E. UCSF Chimera—A visualization system for exploratory research and analysis. *J. Comput. Chem.* **2004**, *25*, 1605–1612. [CrossRef] [PubMed]